Composites Part B 105 (2016) 160–166

Contents lists available at ScienceDirect

Composites Part B

journal homepage: www.elsevier.com/locate/compositesb

Effect of Zinc oxide and Al-Zinc oxide nanoparticles on the rheological properties of cement paste

E. Ghafari [a], S.A. Ghahari [a], Y. Feng [a], F. Severgnini [b], N. Lu [a, *]

[a] Lyles School of Civil Engineering, Sustainable Materials and Renewable Technology (SMART) Lab, Purdue University, USA
[b] School of Electrical and Computer Engineering, Sustainable Materials and Renewable Technology (SMART) Lab, Purdue University, USA

ARTICLE INFO

Article history:
Received 28 March 2016
Received in revised form
27 August 2016
Accepted 29 August 2016
Available online 4 September 2016

Keywords:
ZnO nanoparticles
Rheological properties
Adsorption isotherm
Zeta potential

ABSTRACT

This study aims to evaluate the effect of aluminum doped zinc oxide (AZO) and undoped Zinc oxide (ZnO) nanoparticles addition on the superplasticizer adsorption isotherm and rheological properties of cement paste composites. The adsorption isotherm and zeta potential of pastes containing different proportions of ZnO and AZO nanoparticles were also analyzed. The mechanism of superplasticizer adsorption by nanoparticles was found to be a dominant factor which governs the rheological properties. It was found that the amount of superplasticizer adsorbed increases significantly by incorporating nanoparticles which implies that nanoparticles compete with cement particles to adsorb the polymer. Consequently, the addition of both nanoparticles resulted in a considerable increase in saturation point, yield stress and viscosity values relative to plain cement paste. All mixtures containing 0.4 wt % nanoparticles or lower showed excellent workability retention as compared to the reference mix while, the poor workability retention was observed a higher dosage.

1. Introduction

Nowadays, there is a rapidly growing interest in using nanoparticles in cement and concrete product to tailor materials' mechanical and durability properties [1–6]. The high surface to area ratio of nanoparticles leads to more chemical interactions at the interface, which results in enhanced or novel properties and functions. For instance, the addition of nano SiO_2 and Fe_2O_3 was found to be efficient to improve the mechanical and durability properties of cementitious materials [7–14]. It has been stated that the mechanical properties of high performance concrete can be improved by incorporation of Nano-Al_2O_3 [15]. The addition of Cr_2O_3 nanoparticles can enhance the water permeability resistance of concrete due to refinement of the pore structure [16]. TiO_2 nanoparticles have shown the ability of removing organic pollutants from building facades when exposed to UV radiation [17]. Among the nanoparticles investigated, ZnO has been identified as the most promising one due to its unique materials' photocatalytic and photoluminescence properties [18–21]. ZnO is an inorganic semiconductor compound with a direct band gap of 3.3 eV at room temperature. Similar to TiO_2 as a photocatalyst, the ZnO nanoparticles has been used in self-cleaning applications in concrete structures due to its photocatalytic properties [22–24]. It has been reported that the addition of ZnO improves the reactivity of supplementary cementitious materials, which leads to an increase in the rate of cement hydration and the released heat [25]. Moreover, ZnO addition was found to be effective in reducing the corrosion rate of embedded steel bar in concrete [26]. Although the effect of ZnO nanoparticles on the hydration and hardened state properties of cementitious materials has been explored [27–29], the rheological properties of cement paste containing ZnO has not been investigated. In the present work, attempt has been made to investigate the effect of ZnO nanoparticles on rheological behavior of cement pastes. Adsorption isotherm and zeta potential of pastes containing different proportions of ZnO and AZO nanoparticles were analyzed. In order to compare the results, a plain cement was also considered in the experimental program described ahead. Total organic carbon (TOC) and Zeta potential were measured to further confirm the data.

* Corresponding author.
E-mail address: luna@purdue.edu (N. Lu).

http://dx.doi.org/10.1016/j.compositesb.2016.08.040
1359-8368/Published by Elsevier Ltd.

2. Experimental program

2.1. Materials

The cement paste mixtures were prepared using the following main constituents: Portland cement type I 42.5 R (C); polycarboxylate ether based superplasticizers (SP); and two different types of ZnO nanoparticles including undoped ZnO nanoparticle (ZnO) and aluminum doped ZnO nanoparticle (AZO). Table 1 shows some physical and chemical properties of cement. The adopted chemical admixture was a polycarboxylic acid based superplasticizer (SP) with the density of 1.108 g/cm^3. The properties of ZnO and AZO nanoparticles are presented in Table 2. The cement pastes were prepared in this study by using a vacuum mixer to reduce the entrapped air voids in the mixes.

Table 3 presents the eleven series of mixtures, prepared with ZnO, AZO and a reference mixture without nanoparticles. Nanoparticles were incorporated as cement replacement by 0.2, 0.4, 0.6, 0.8 and 1 by wt. % of cement. The total content of powder was kept constant in volume. In addition, the water to binder ratio was fixed at 0.35 for all the mixtures.

2.2. Zeta potential measurement

The effect of different dosages of superplasticizer on the zeta potential of cement suspensions was determined with a Colloidal Dynamics Acoustosizer IIs. The systems measure zeta potential using electrophoretic light scattering. Cement suspensions were prepared by mixing 30 g of binder with 160 g of water (solid fraction in the suspension = 0.16). After stirring for 15 min in a magnetic stirrer, the suspensions were placed in a sonicator for 5 min and then in the measuring cell to determine their zeta potential. Polycarboxylate admixture dosages ranging from 0 to 7 mg polymer/g cement were added to these suspensions using an automatic titrator. The zeta potential values were corrected for the pore solution background contribution. Diluted solutions were used in order to study the interaction between PCE-cement from a colloidal chemical point of view.

2.3. Adsorption isotherm

In order to determine the superplasticizer adsorption isotherms, the same mix design for rheology tests were used. The pore solution of the cement paste was centrifuged, the liquid phase was removed through a 0.45 lm Nylon filter by air pressure filtration and the total organic carbon content was found by a SHIMADZU TOC-VCSH/CSN total organic carbon (TOC) analyzer.

2.4. Rheological measurement

The coaxial Anton Paar MCR 302 Rheometer was used to assess the rheological properties of cement pastes. The inner cylinder rotates at different velocities, while the outer cylinder remains stationary. The resulting torque was registered at the inner cylinder. The rheological properties of each cement paste were determined using the following testing procedure. At the start of each test, the cement paste was pre-sheared for 60 s at the maximum shear rate employed during the test, which is 100 s^{-1}. After the pre-shearing period, the cement paste was subjected to a stepwise decrease in shear rate from 100 to 2 s^{-1} in 11 steps. The rheological properties were measured at 15, 45, 75 and 90 min. Also the static yield stress was measured at 28, 43, 58, 73 and 88 min. The testing procedure is illustrated in Fig. 1. The rheological properties of cement-based materials are usually characterized with the Bingham model (Eq. (1)):

$$\tau = \tau_0 + \mu_p \cdot \dot{\gamma} \quad \text{(Eq.1)}$$

For this equation, τ is the shear stress (Pa), τ_0 is the yield stress (Pa), μp is the plastic viscosity (Pa s), and $\dot{\gamma}$ is the shear rate (s-1). The yield stress is the stress needed to start the flow. This means that applying a stress lower than the yield stress will not cause any flow in the material. The plastic viscosity is the resistance of the material to an increase in flow rate once the yield stress is exceeded. The yield stress and the plastic viscosity are the two Bingham parameters that characterize the flow properties of the studied materials. When the rheological measurement is performed with a coaxial cylinder rheometer, torque (T) and rotational velocity (N) are measured. Shear stress and shear rate data must be derived from the torque and rotational velocity data. When the torque is at equilibrium at each shear rate step, the rheological properties can be calculated by means of the Reiner-Riwlin equation. If the torque was not at equilibrium at a certain step, the respective data point was eliminated from the results.

The Reiner-Riwlin equation transforms the parameters G and H (Eq. (2)), defining a linear relationship between T and N, into the Bingham parameters (Eqs. (3) and (4)). This assumes a laminar, stable flow and no particle movements in the horizontal or vertical direction and also material, in the entire gap is sheared [30].

$$T = G + H \cdot N \quad \text{(Eq.2)}$$

$$\tau_0 = \frac{G}{4\pi h} \cdot \left(\frac{1}{R_i^2} - \frac{1}{R_o^2} \right) \cdot 1/ln(R_o/R_i) \quad \text{(Eq.3)}$$

$$\mu_p = \frac{H}{8\pi^2 h} \cdot \left(\frac{1}{R_i^2} - \frac{1}{R_o^2} \right) \quad \text{(Eq.4)}$$

where R_i is the inner cylinder (m), R_o is the outer cylinder (m), and h is the height of the cylinder (m).

The static yield stress when a concentric cylinder rheometer is employed, can be calculated using Eq. (5) [31]:

$$\tau_s = \frac{T}{2\pi r^2 h} \quad \text{(Eq.5)}$$

where τ_s = static yield stress (Pa) and r = radial parameter (m) and corresponds to the spread between inner radius R_i and outer radius R_o.

Table 1
Chemical composition and physical properties of cement.

Chemical analysis (wt %)	Cement
SiO_2	20.9
Al_2O_3	4.60
Fe_2O_3	3.15
CaO	62.0
MgO	2.00
SO_2	3.60
K_2O	<1
Na_2O	<1
Specific gravity	3.14

3. Results and discussion

3.1. Zeta potential

The stability of the colloidal system is a function of the zeta

Table 2
Properties of ZnO nanoparticles.

Formula	Aluminum doped	Specific surface area (m^2/g)	Purity	Crystal phase	Mean diameter (nm)	Density (g/cm3)
ZnO	0	54 ± 20	>99.9 (wt %)	Zincite (hexagonal)	20 ± 5	5.6
AZO	0.2 (wt %)	54 ± 20	>99.9 (wt %)	Zincite (hexagonal)	20 ± 5	5.6

Table 3
Composition of pastes mixture (by weight, g/cm3).

		Cement	Water	SP	ZnO	AZO
Ref	PC	593.9	207.9	2.4	0	0
ZnO Mixtures	ZnO1	592.7	207.9	2.4	1.18	0
	ZnO2	591.5	207.9	2.4	2.37	0
	ZnO3	590.3	207.9	2.4	3.56	0
	ZnO4	589.1	207.9	2.4	4.75	0
	ZnO5	587.9	207.9	2.4	5.93	0
AZO Mixtures	AZO1	592.7	207.9	2.4	0	1.18
	AZO2	591.5	207.9	2.4	0	2.37
	AZO3	590.3	207.9	2.4	0	3.56
	AZO4	589.1	207.9	2.4	0	4.75
	AZO5	587.9	207.9	2.4	0	5.93

3.2. Adsorption isotherms

The compatibility of cement paste with chemical admixture highly depends on the amount of polymer adsorbed onto the cement. This adsorption isotherm can be further related to the rheological properties of cement paste. In this study the adsorption isotherm was measured in two major steps. At the first step the saturation point for both nanoparticles and cement was determined. The second step studied the effect of different amount of nanoparticles on the amount of SP adsorption. The saturation dosage was determined as the dosage of SP, beyond which the adsorption rate did not substantially varied. At each step, SP/binder

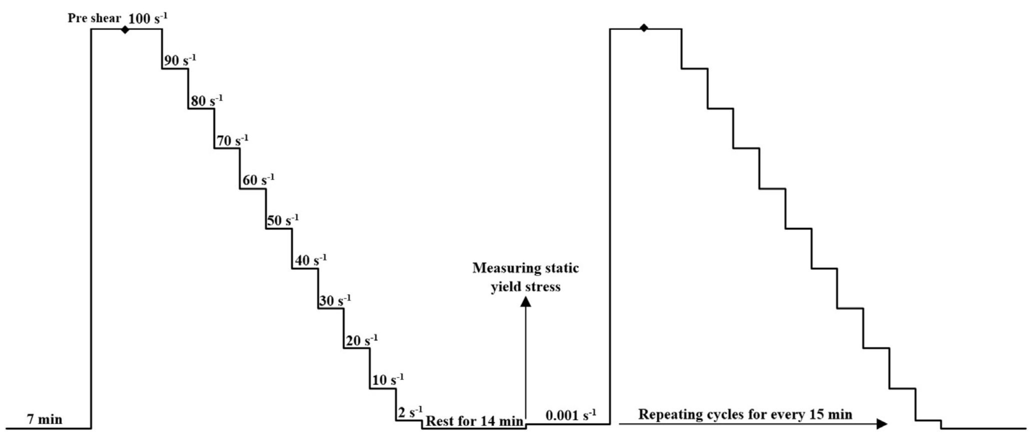

Fig. 1. The rheology testing procedure.

potential. Therefore, the determination of zeta potential enables the study of the action mechanism of admixtures, since the adsorption of SP on the solid surface of binder modifies the surface charge of the particles [32]. The variations in Zeta potential for ZnO and AZO versus the SP content is presented in Fig. 2. The zeta potential of pure cement paste was found to be about −10 mV. The gradual addition of SP led to a decrease in the zeta potential values of both ZnO and AZO suspensions, indicating the effective interaction between SP and nanoparticles. In fact, Polycarboxylate SP is a negatively charged polyelectrolyte, therefore its adsorption onto particles results in a zeta potential reduction. The AZO suspension exhibited higher values of zeta potential than ZnO suspension and plain cement.

However, as shown, no significant change of zeta potential in various composites with a function of SP volume added. In general, the higher this potential is with the same polarity, the stronger the adsorption between particles and SP is expected [33,34]. However, as shown, no significant change of zeta potential was observed in various composites with a function of SP volume added, which indicated that repulsive potential that resulted from electrostatic interactions was negligible. Therefore, the steric hindrance caused by the draft side chains of the polymer, plays a dominant role compared to electric repulsion in the dispersing of cement particles [35].

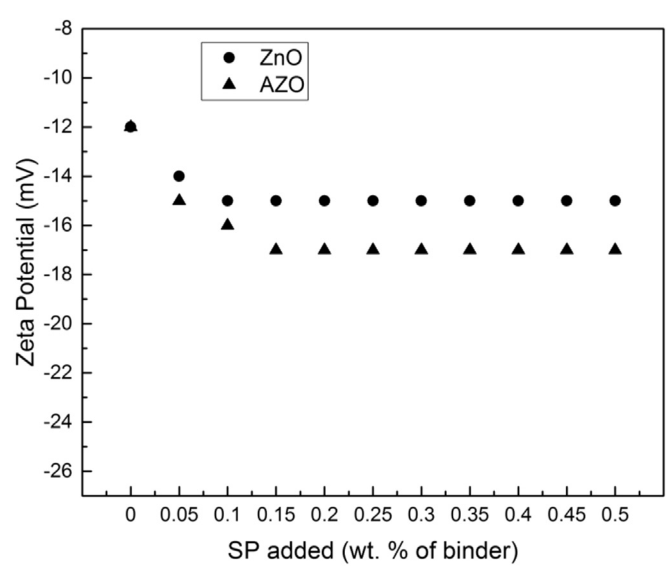

Fig. 2. Superplasticizer adsorption isotherms and variation in the zeta potential.

was increased per 0.05% by weight of total binder and the amount of adsorbed SP was measured. The results indicated that both nanoparticles exhibited higher saturation point compared to cement. As presented in Fig. 3, for plain cement pastes, the saturation dosage of 0.25% by mass of binder was obtained. However, the obtained admixture saturation dosage for ZnO and AZO was 0.4 and 0.45 respectively. The higher adsorption of nanoparticles might be due to its higher specific surface area of nanoparticles. Fig. 4 presents the isotherms for the polycarboxylate SP adsorbed versus the amount of nanoparticles addition. The results indicated that the amount of SP adsorbed increases linearly with the increase of nanoparticles, however after a certain SP content, the adsorbed amount reached the maximum beyond which remains almost constant. AZO suspension exhibited higher adsorption rate than ZnO, which can be due to higher induced zeta potential on the particle surface. The obtained TOC results were in a good agreement with the zeta potential data.

3.3. Rheological properties

The rheological properties including yield stress and viscosity were calculated using Bingham model. These parameters can further be used to optimize the mixture proportions to produce the desired degree of flow and segregation resistance in concrete [36]. As presented in Table 3, the amount of SP was kept constant in all the mixtures, in order to avoid the effect of such factor on the rheological properties. The evolution of yield stress and viscosity of the pastes containing ZnO and AZO as function of time are presented in Fig. 5 and Fig. 6, respectively. As compared to the plain cement (reference mixture), the addition of both ZnO and AZO resulted in a considerable increase in yield stress and viscosity. The higher value of yield stress and viscosity can be attributed to two main reasons. First, the addition of nanoparticles significantly increases the water demand of cement paste mixture due to the higher specific surface area. Therefore, a considerable amount of water in the mix was absorbed by nanoparticles, leading to a significant decrease in workability. As a consequence, there was no sufficient water available for lubrication allowing particles free movement so that the higher shear stress was required to breakdown the cement paste structures, which resulted in a higher yield stress and viscosity [37,38]. Secondly, according to TOC data,

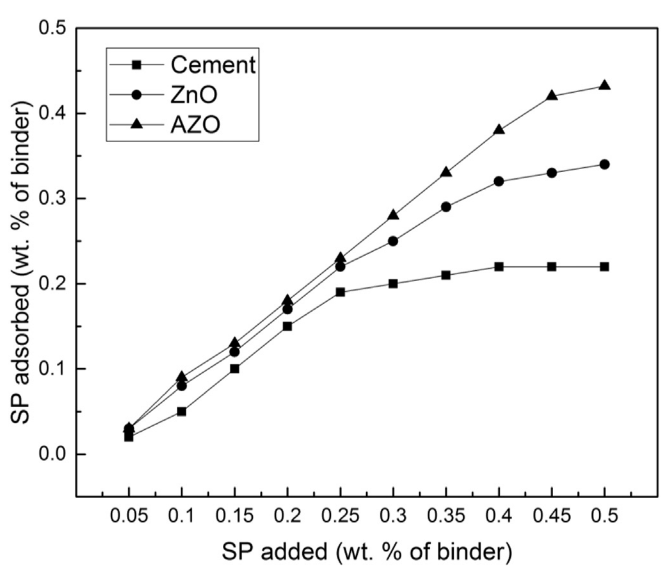

Fig. 3. Adsorption isotherms of cement, ZnO and AZO.

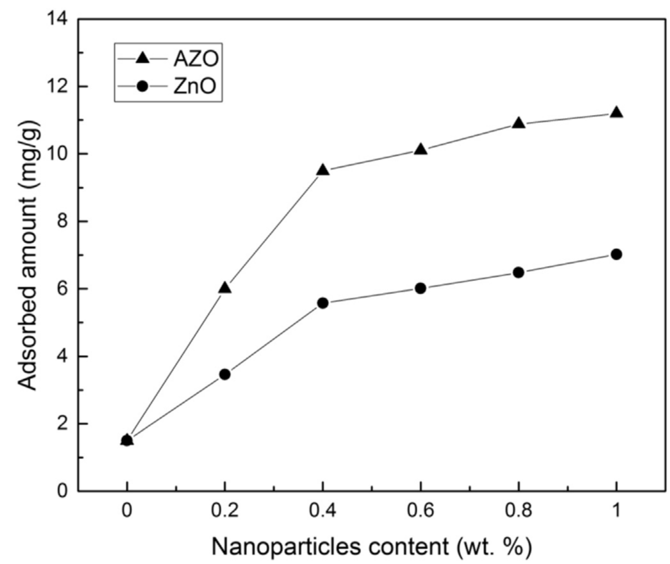

Fig. 4. Effect of nanoparticle addition on the adsorption of SP.

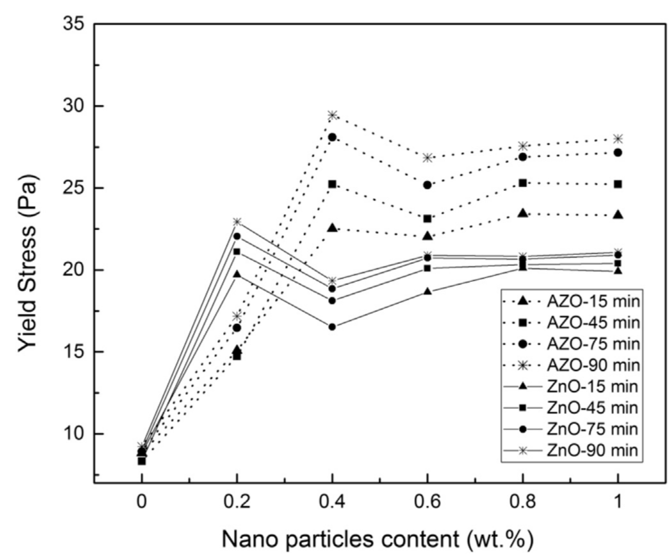

Fig. 5. The evolution of yield stress vs time of cement paste containing ZnO and AZO.

cement and Zinc oxide nanoparticles could compete to adsorb polymers which leave less SP available for adsorption by cement particles to be efficiently dispersed [39]. By comparing the effect of both types of nanoparticles on the rheological properties, it can be observed that AZO exhibited higher yield stress and viscosity resulted in a stiffer mix compare to pastes containing ZnO. This behavior can be attributed to higher adsorption isotherm of AZO compare to ZnO. The results indicated that the addition of AZO beyond 0.4 wt %, yield approximately the same value of fluidity (Figs. 5 and 6). This behavior can be seen in adsorption isotherm data obtained by TOC method, in which the adsorbed isotherm amount of SP by AZO suspension didn't vary after 0.4 wt % content. This clearly implies that the mechanism of isotherm adsorbed SP by nanoparticles governs the rheological properties of cement pastes. For the mixture containing ZnO, the evolution of rheological properties was found to be similar to AZO-pastes.

In order to study the thixotropic behavior, the static yield stress of AZO and ZnO mixtures were also measured. Thixotropy is the

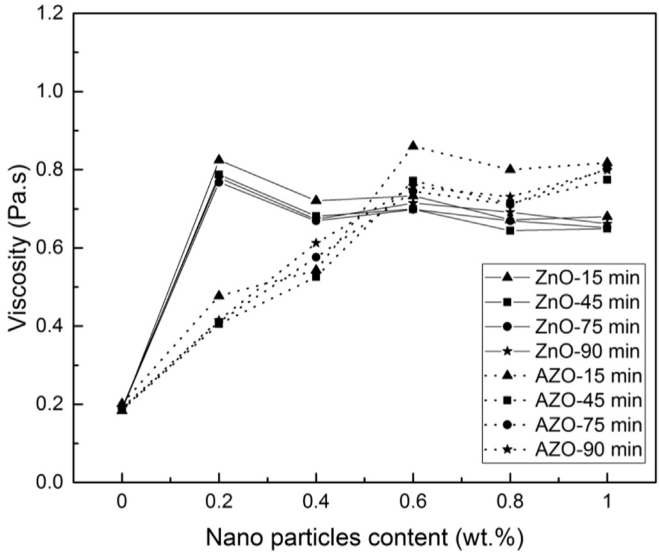

Fig. 6. The evolution of viscosity vs time of cement paste containing ZnO and AZO.

reversible decrease in stress under shear and build-up at rest due to physical effects. During the static yield stress measurements, the torque of the vane necessary to obtain a constant rotational velocity of 0.001 rps was measured at 28, 43, 58, 73, and 88 min after first contact of cement and water. As the imposed rotational velocity was sufficiently low, different static yield stress measurements could be performed at different times assuming that the sample remained at rest the entire time. The static yield stress assumed to be the peak yield stress of the diagram, calculated assuming that the concrete within the vanes behaves like a rigid cylinder, and all the shearing happens across a cylindrical surface surrounding the vane [40]. In order to avoid the influence of experimental scatter, the peak torque was calculated as the peak of a polynomial fit around the experimental data surrounding the peak torque. The static yield stress results of AZO and ZnO is shown in Fig. 7. The results indicated that the addition of AZO and ZnO led to an increase in static yield stress relative to the plain cement. The static yield stress showed a clear increase with time, indicating the thixotropic behavior of the cement pastes. As shown, the increase in static yield stress with time is clearly influenced by the amount of AZO and ZnO, because the higher amount of nanoparticle causes a faster thixotropic build-up. In general, the evolution of static yield stress for both AZO and ZnO mixture pastes was found to be similar to dynamic yield stress in which after the maximum value the static yield stress didn't show a significant change.

The rheological properties were followed with time to investigate the workability retention. The main objective of this task is to understand the workability loss of the cement pastes with time, as a function of the use of different nanoparticle dosages. In this study, the average rate of dynamic yield stress and plastic viscosity change over 90 min has been calculated. The method of calculation for plastic viscosity is as following. First the change of rheological properties at 30, 45, 60, 75 and 90 min has been obtained by taking the difference between the newly measured plastic viscosity and the previous value, divided by the time lapse (15 min). Finally, the average rate of change of the dynamic yield stress and plastic viscosity were determined by calculating the average of the five previously obtained values using Eq. (6) and Eq. (7) respectively.

$$\Delta\tau_0/\Delta t = \frac{\Delta\tau_0/\Delta t_{30} + \Delta\tau_0/\Delta t_{45} + \Delta\tau_0/\Delta t_{60} + \Delta\tau_0/\Delta t_{75} + \Delta\tau_0/\Delta t_{90}}{5} \quad \text{(Eq.6)}$$

$$\Delta\mu_p\Big/\Delta t = \frac{\Delta\mu_p\Big/\Delta t_{30} + \Delta\mu_p\Big/\Delta t_{45} + \Delta\mu_p\Big/\Delta t_{60} + \Delta\mu_p\Big/\Delta t_{75} + \Delta\mu_p\Big/\Delta t_{90}}{5} \quad \text{(Eq.7)}$$

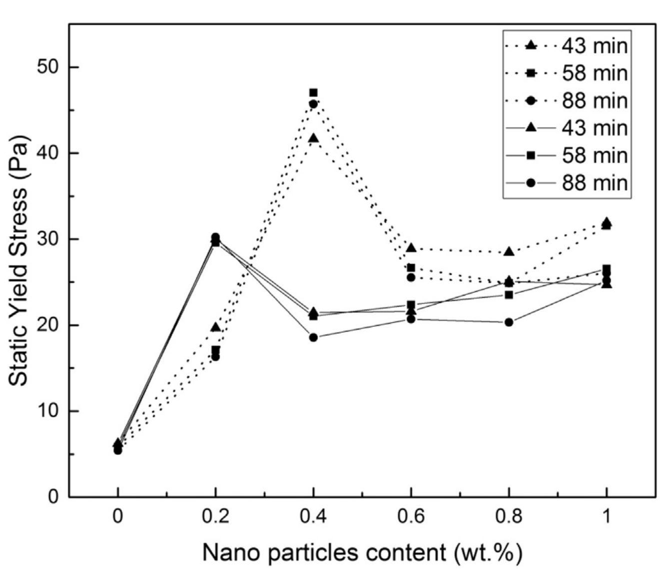

Fig. 7. The evolution of static yield stress vs time of cement paste containing ZnO and AZO.

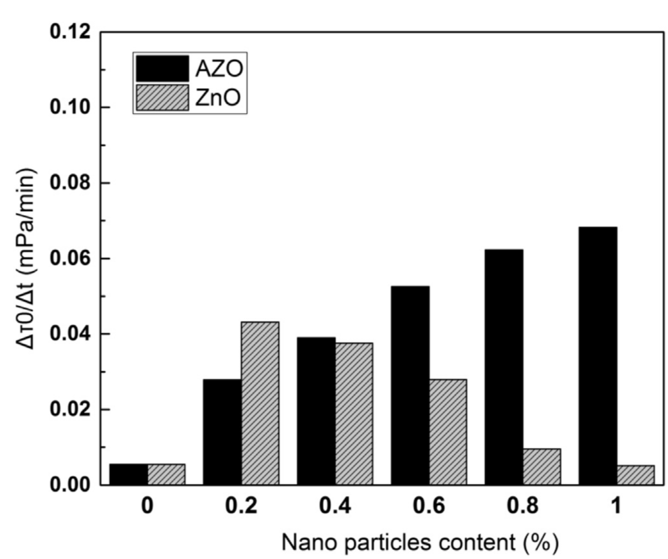

Fig. 8. Yield stress retention of pastes containing different dosage of ZnO and AZO.

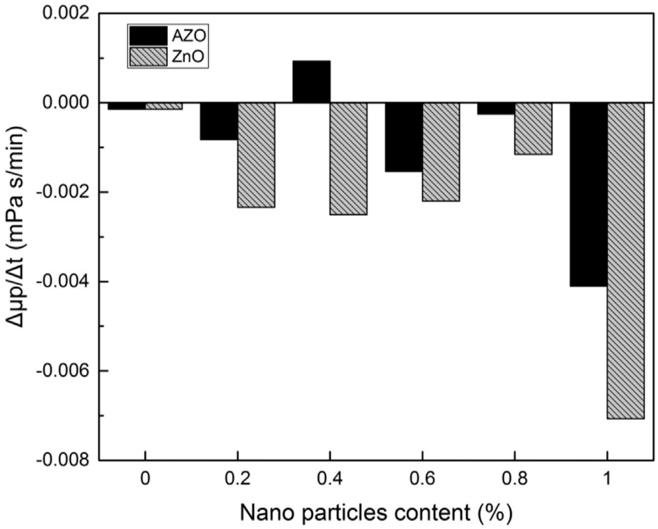

Fig. 9. Viscosity retention of pastes containing different dosage of ZnO and AZO.

The effect of both AZO and ZnO on workability retention are shown in Fig. 8 and Fig. 9 respectively. As shown in Fig. 8, the addition of AZO up to 0.6 wt % led to an increase in the yield stress over the time, however, the paste containing more than 0.6 wt % AZO showed poor fluidity retention. On the other hand, the pastes containing ZnO showed excellent fluidity retention even at higher dosage. Fig. 9 shows the effect of the addition of ZnO nanoparticle on the viscosity retention through the time. The results indicated a distinctive behavior, in which the addition of ZnO resulted in a poor viscosity retention. In general, all mixtures containing 0.4 wt % nanoparticles or lower showed excellent workability retention as compared to the reference mix while, the poor workability retention was observed at higher dosage.

4. Conclusion

In this study, the effect of two different Zinc oxide nanoparticles on the adsorption isotherm and rheological properties of the cement pastes were studied. It was found that the amount of SP adsorbed increases significantly by incorporating nanoparticles which implies that nanoparticles compete with cement particles to adsorb the polymer. Both nanoparticles exhibited higher adsorption rate compare to cement, due to the higher specific surface area. This behavior resulted in a lower available SP in the mixture so that the addition of ZnO nanoparticle resulted in a considerable increase in saturation point, yield stress and viscosity relative to plain cement paste. AZO suspension exhibited higher adsorption rate than ZnO which can be due to the higher induced zeta potential on the particle surface. The rheological properties were found to be in a good agreement with the adsorption isotherm and zeta potential data. The mechanism of SP adsorption by nanoparticles was found to be a dominant factor that governs the rheological properties. Also, the increase in static yield stress with time is affected by the amount of ZnO and AZO in which higher amount of nanoparticle causes a faster thixotropic build-up. The workability retention results indicated that the pastes containing AZO exhibited better performance in terms of viscosity retention, while the addition of ZnO was found to be more effective in fluidity retention. All mixtures containing 0.4 wt % nanoparticles or lower showed excellent workability retention compared to the reference mix while, the poor workability retention was observed at higher dosage.

Acknowledgement

The authors would like to thank Prof. Maria Santagata and Prof. Andrew Whelton at Purdue University for their kind support to provide the rheometer and TOC device.

References

[1] Stefanidou M, Papayianni I. Influence of nano-SiO2 on the Portland cement pastes. Compos Part B Eng 2012;43(6):2706–10.
[2] Mohamed SAE-A, Abd El-Rahman Ragab. Physico-mechanical properties and microstructure of blended cement incorporating nano-silica. Int J Eng Res Technol 2014;3(7):339–58.
[3] Hakamy A, Shaikh FUA, Low IM. Characteristics of nanoclay and calcined nanoclay-cement nanocomposites. Compos Part B Eng 2015;78:174–84.
[4] Abd El-Aleem S, Abd El-Rahman Ragab. Chemical and physico-mechanical properties of composite cements containing micro- and nano-silica. Int J Civ Eng Technol 2015;6(5):45–64.
[5] El-Didamony H, Abd El-Aleem S, Abd El-Rahman Ragab. Hydration behavior of composite cement containing fly ash and nanosized-SiO2. Am J Nano Res Appl 2016;4(2):6–16.
[6] Ghafari E, Costa H, Júlio E. Critical review on eco-efficient ultra high performance concrete enhanced with nano-materials. Constr Build Mater 2015;101(Part 1):201–8.
[7] Qing Y, Zenan Z, Deyu K, Rongshen C. Influence of nano-SiO 2 addition on properties of hardened cement paste as compared with silica fume. Constr Build Mater 2007;21(3):539–45.
[8] Li H, Xiao H, Yuan J, Ou J. Microstructure of cement mortar with nano-particles. Compos Part B Eng 2004;35(2):185–9.
[9] Heikal M, Abd El-Aleem S, Morsi WM. Characteristics of blended cements containing nano-silica. HBRC J 2013;9(3):243–55.
[10] Abd El-Aleem S, Heikal M, Morsi WM. Hydration characteristic, thermal expansion and microstructure of cement containing nano-silica. Constr Build Mater 2014;59(0):151–60.
[11] Najigivi A, Khaloo Alireza, Iraji zad Azam, Abdul Rashid Suraya. Investigating the effects of using different types of SiO2 nanoparticles on the mechanical properties of binary blended concrete. Compos Part B Eng 2013;54:52–8.
[12] Shiri S, Abbasi MH, Monshi A, Karimzadeh F. A study on mechanical and physical properties of monocalcium aluminate cement reinforced with nano-SiO2 particles. Compos Part B Eng 2014;56:30–3.
[13] García-Taengua E, Sonebi M, Hossain KMA, Lachemi M, Khatib J. Effects of the addition of nanosilica on the rheology, hydration and development of the compressive strength of cement mortars. Compos Part B Eng 2015;81:120–9.
[14] Ghafari E, Arezoumandi M, Costa H, Júlio E. Influence of nano-silica addition on durability of UHPC. Constr Build Mater 2015;94:181–8.
[15] ASTM C39/C39M-15a. Standard test method for compressive strength of cylindrical concrete specimens. 2015.
[16] ASTM C469/C469M-14. Standard test method for static modulus of elasticity and Poisson's ratio of concrete in compression. 2014.
[17] Lee BY, Kurtis KE. Influence of TiO2 nanoparticles on early C3S hydration. J Am Ceram Soc 2010;93(10):3399–405.
[18] Houšková V, Štengl V, Bakardjieva S, Murafa N, Kalendova A, Opluštil F. Zinc oxide prepared by homogeneous hydrolysis with thioacetamide, its destruction of warfare agents, and photocatalytic activity. J Phys Chem A 2007; 111(20):4215–21.
[19] Xu F, Zhang P, Navrotsky A, Yuan Z, Ren T, Halasa M, et al. Hierarchically assembled porous ZnO nanoparticles: synthesis, surface energy, and photocatalytic activity. Chem Mater 2007;19(23):5680–6.
[20] Kumar B, Kim S-W. Energy harvesting based on semiconducting piezoelectric ZnO nanostructures. Nano Energy 2012;1(3):342–55.
[21] Wang ZL. Energy harvesting for self-powered nanosystems. Nano Res 2008;1(1):1–8.
[22] Kenanakis G, Vernardou D, Katsarakis N. Light-induced self-cleaning properties of ZnO nanowires grown at low temperatures. Appl Catal A General 2012;411–412:7–14.
[23] Khayyat SA, Abaker M, Umar A, Alkattan M, Alharbi N, Baskoutas S. Synthesis and characterizations of Cd-doped ZnO multipods for environmental remediation application. J Nanosci Nanotechnol 2012;12(11):8453–8.
[24] Copeland LE, Kantro DL, Verbeck GJC. Chemistry of hydration of portland cement. In: cement chemistry. Cement and Concrete Association; 1960.
[25] Taylor-Lange SC, Riding KA, Juenger MCG. Increasing the reactivity of metakaolin-cement blends using zinc oxide. Cem Concr Compos 2012;34(7): 835–47.
[26] Troconis de Rincón O, Pérez O, Paredes E, Caldera Y, Urdaneta C, Sandoval I. Long-term performance of ZnO as a rebar corrosion inhibitor. Cem Concr Compos 2002;24(1):79–87.
[27] Gawlicki M, Czamarska D. Effect of ZnO on the hydration of Portland cement. J Therm Analysis 1992;38:2157–61.
[28] Ataie FF, Juenger MCG, Taylor-Lange SC, Riding KA. Comparison of the retarding mechanisms of zinc oxide and sucrose on cement hydration and interactions with supplementary cementitious materials. Cem Concr Res 2015;72:128–36.

[29] Nochaiya T, Sekine Y, Choopun S, Chaipanich A. Microstructure, characterizations, functionality and compressive strength of cement-based materials using zinc oxide nanoparticles as an additive. J Alloys Compd 2015;630:1–10.
[30] Feys D, Wallevik JonE, Yahia Ammar, Khayat KamalH, Wallevik OlafurH. Extension of the Reiner–Riwlin equation to determine modified Bingham parameters measured in coaxial cylinders rheometers. Mater Struct 2013;46(1–2):289–311.
[31] Wallevik OH, Feys Dimitri, Wallevik Jon E, Khayat Kamal H. Avoiding inaccurate interpretations of rheological measurements for cement-based materials. Cem Concr Res 2015;78(Part A):100–9.
[32] Srinivasan S, Barbhuiya SA, Charan D, Pandey SP. Characterising cement–superplasticiser interaction using zeta potential measurements. Constr Build Mater 2010;24(12):2517–21.
[33] Zingg A, Winnefeld F, Holzer L, Pakusch J, Becker S, Figi R, et al. Adsorption of polyelectrolytes and its influence on the rheology, zeta potential, and microstructure of various cement and hydrate phases. J Colloid Interface Sci 2008;323(2):301–12.
[34] Zingg A, Winnefeld F, Holzer L, Pakusch J, Becker S, Figi R, et al. Interaction of polycarboxylate-based superplasticizers with cements containing different C3A amounts. Cem Concr Compos 2009;31(3):153–62.
[35] Yoshioka K, Sakai E, Daimon M, Kitahara A. Role of steric hindrance in the performance of water-reducers for concrete. J Am Ceram Soc 1997;80(10):2667–72.
[36] Wallevik Ó. Rheology – a scientific approach to develop self-compacting concrete. In: International RILEM symposium on self-compacting concrete. RILEM Publications; 2003.
[37] Korpa A, Trettin R. Ultra high performance cement-based composites with advanced properties containing nanoscale pozzolans. In: Proceedings of the second international symposium on ultra high performance concrete; 2008 [Kassel, Germany].
[38] Ghafari E, Costa H, Júlio E, Portugal A, Durães L. The effect of nanosilica addition on flowability, strength and transport properties of ultra high performance concrete. Mater Des 2014;59:1–9.
[39] Alonso MM, Palacios M, Puertas F. Compatibility between polycarboxylate-based admixtures and blended-cement pastes. Cem Concr Compos 2013;35(1):151–62.
[40] Yan J, James AE. The yield surface of viscoelastic and plastic fluids in a vane viscometer. J Newt Fluid Mech 1997;70(3):237–53.